Study of evolution of trapped particle undamped coherent structures: An important agent in intermittent plasma turbulence and anomalous transport

Debraj Mandal, Devendra Sharma

Institute for Plasma Research, Bhat, Gandhinagar, 382428, India

Hans Schamel

Physikalisches Institut, Universität Bayreuth, D-95440 Bayreuth, Germany

The physics of particle and energy transport in collision-less plasmas presents substantial challenge because of largely linear threshold based plasma turbulence are replaced by their nonlinear counterparts capable of operating at smaller amplitudes. An outstanding property for collisionless plasmas is the essential nonlinear character of coherent structures supported by them at small amplitude. A supplementary mode spectrum of stable coherent structure plays an important role in intermittent plasma turbulence and anomalous transport. In the present work, these additional undamped structures are considered, in a 1D, collision-less plasma as a paradigm of intermittent plasma turbulence and anomalous transport and are investigated based on the result of a kinetic simulation of the plasma. The computational analysis explores initial eddy-like,non-topological electron phase-space seed fluctuation in a current-driven plasma within the linear threshold limit for accessing the regime uncovered under the linear approximation. After a (transient) transition phase modes of the privileged spectrum of cnoidal modes are excited which in the present case consist of a solitary electron hole (SEH), two counter-propagating “Langmuir” modes (plasma oscillation), and an ion acoustic mode. A quantitative explanation involves a nonlinear dispersion relation with a forbidden regime and the negative energy character of the SEH, properties being inherent in Schamel's model of undamped Vlasov-Poisson structures identified here as lowest order trapped particle equilibria. An important role in the final adaption of nonlinear plasma eigenmodes is played by a deterministic response of trapped electrons which facilitates transfer of energy from electron thermal energy to an ion acoustic nonuniformity, accelerating the SEH and positioning it into the right place assigned by the theory.

I. INTRODUCTION

Trapped particle nonlinearity generated coherent structures are the important agent in collision less plasma turbulence and anomalous transport. Coherent structures are generated due to competition between the nonlinearity and the dispersiveness property of plasma. According to linear theory of plasma amplitude based fluid nonlinearity appear at high amplitude limit hence coherent structures are generated only at higher amplitude perturbation. But in collision-less plasmas trapped-particle nonlinearity acts at very small amplitude limit which generates coherent structures. When ion temperature is nearly equal or smaller than electron temperature then linear theory of plasma predicts ion acoustic waves are stable unless the drift velocity between electron and ion exceed a certain critical value [1; 2]. Drift bellow this critical limit is called subcritical regime of plasmas. As a consequence in last few decades ion acoustic turbulence in subcritical regime does not receive much attention in the context of magnetically confined fusion plasma. In this paper, hence a subcritically-driven, 1D, collisionless plasma as a paradigm of driven intermittent plasma turbulence and anomalous transport is considered with the focus on undamped coherent electrostatic structures, mainly electron hole. Subcritically driven turbulence of plasma state often presenting its strong signatures in nature [3; 4], experiments [5–7] and in simulations [8–13] of collisionless hot plasmas. Underlying this are instabilities of nonlinear collective eigenmodes of nonthermal distributions rather than those of the normal linear eigenmodes of a thermalized distribution f_0. The linear plasma modes are recoverable by selecting the corresponding poles of dispersion function to perform the contour integral along Landau contour which yields $f_0' \equiv \partial f_0/\partial v$ as a unique driver for the growth of the plasma modes and only source of microinstabilites. However stability is a nonlinear issue and the growth process of phase space structures circumvent linear theory and require nonlinear basis. Explanation of this stronger nonlinear basis of the turbulence threshold is explored both by stochastic [11; 14] as well as deterministic approaches [15; 16], prescribing the growth largely linked to species' f'. With these criteria often defied by the evolution, no basis is known for quantitatively exploring drivers of rather complex unstable subcritical evolution [17] of coherent phase-space perturbations constituting fundamental nonlinear collective eigenmodes in hot nonthermal collisionless plasma [18], inevitably unstable if they possessed a forbidden regime or violated the negative energy state condition [19] in certain regimes. By first recovery of these two characteristic electron hole attributes in our simulations, we have quantitatively applied, to the observed evolution, a formulation implementing a stochastic scale cut-off to approach fundamental smallest nonlinear unit of phase-space perturbations [20]. We have thus characterized the subcritcally unstable response in terms of parameters that allow generalization to ensembles, or large scale nonthermal phase-space equilibria.

We present results of two cases of high-resolution Vlasov simulations initialized with small phase-space perturbations capable of developing into unstable hole structures. A forbidden regime is identified for the electron holes (EHs) where they accelerate providing evidence of their multifaceted sub-critical nonlinear instability [17; 21], growing coherent structures. The second part of observations shows that the electron holes can also be destabilized by parametric coupling to conventional collective modes of collisionless plasmas. In all cases the phase velocity v_0 of the finally settled SEH exceeds the electron drift and is hence located at the right wing of f_{e0}, which has a negative slope that, according to standard wave theory, would imply disappearance by Landau damping [22]. We hence have observed a nonlinear evolution beyond the generally accepted Landau scenario for the plasma turbulence.

II. VLASOV SIMULATION OF TRAPPED PARTICLE STRUCTURE DEVELOPMENT

In the 1-D Vlasov-Poisson simulation with exact mass ratio ($\delta = m_e/m_i = 1/1836$), a well localized eddy-like initial electron distribution perturbation has been used which has the following analytic form,

$$f_1(x,v) = -\epsilon \,\mathrm{sech}\left[\frac{v-v_1}{L_1}\right] \mathrm{sech}^4[k(x-x_1)] \tag{1}$$

where ϵ is the amplitude of the perturbation, L_1 is the width of the perturbation in the velocity dimension and k^{-1} is its spatial width. We use the Debye length λ_D, inverse electron plasma frequency ω_{pe}^{-1} and electron thermal velocity $v_{the} = \sqrt{T_e/m_e}$ as normalizations for length, time and electron velocities, respectively. The background electron and ion velocity distributions are Maxwellian with a finite electron drift v_D,

$$f_{0e}(v) = \frac{1}{\sqrt{2\pi}} \exp\left[-\frac{(v-v_D)^2}{2}\right] \tag{2}$$

$$f_{0i}(u) = \frac{1}{\sqrt{2\pi}} \exp\left[-\frac{u^2}{2}\right] \tag{3}$$

where $u = \sqrt{\theta/\delta}\, v$ and $v_D = 0.01$ is chosen below the critical linear threshold $v_D^* = 0.053$ [2] for $\theta = T_e/T_i = 10$ used by us.

We first present the evolution of the total electron distribution $f_e = f_{0e} + f_1$ for two cases with $v_1 = 0.05$ and 0.01, respectively, i.e., the perturbation located beyond the maximum of $f_{0e}(v)$ far in the decreasing tail in case 1, just at its maximum in case 2. It is additionally initiated from the center, $x = 15$, of the simulation box of length $L = 30$. The phase-space widths of the perturbation is chosen as $L_1 = 0.01$ along v and $k^{-1} = 10$ along x in expression (1) with the perturbation strength $\epsilon = 0.06$.

Despite the fact that we are well in the linearly Landau damped region we expect the nonlinear excitation of an electron hole mode (EH), as suggested by our previous publication [17]. This EH is indeed recovered (Fig. 1) in case 1 (apart from a completely decoupled undamped electron plasma oscillation in both the cases) where a much faster saturation of ion expulsion (potential decay) is achieved resulting in an immediate set up of a coherently propagating structure. For the second case the slower perturbation, however, the phase-space structure presented in left column of Fig. 2, seen accelerating to a higher velocity after a noticeable change in its topology in the phase-space. For all these cases, the removal of electrons ($f_1 \ll f_0$) from a small velocity interval translates in an electron density dip (potential hump) at x_1, instantly introducing a phase-space separatrix about (x_1, v_1). A slowly varying separatrix corresponds to an adiabatic invariant, with a response time (time for it to modify) longer than that of untrapped ions ($\tau_{\mathrm{adiabatic}} \gg \omega_{ip}^{-1}$). While ions can be expelled faster to restore quasineutrality, an inward flux of them is also expected, driven by deficiency of thermal electrons at x_1 that must allow ions to easily bunch at x_1 [23]. Clearly, in a stably propagating solitary electron-hole structure, these two fluxes must balance and a comoving ion density hump must exist, as seen in Fig. 1(j). However, an unstable, subcritically evolving and accelerating perturbation recovered in Figs. 2, in clear contrast to Fig. 1, is subject of this paper.

Note that in both the cases the u_1's are sufficiently large (6.78 and 1.36 v_{thi}), to neglect ion trapping in first approximation. However, since the ion sound speed $c_s = 3.16 v_{thi}$, in case 1 the perturbation is moving supersonically, in cases 2 we have subsonic propagation. This implies that the ion mobility can be largely neglected in case 1 but plays an important role in cases 2. Consequently, the time scales of the evolution are rather distinct in all the cases, being determined essentially by ω_{pe}^{-1} for case 1 where the electron hole has settled in about 10 ω_{pe}^{-1}, but by ω_{pi}^{-1} for case 2, where the settling occurs in about 3.6 $\omega_{pi}^{-1} \approx 156\omega_{pe}^{-1}$.

In the simulation f_1 represents tiny granular patches of shear flow in phase space representing individual particle configurations (fine texture) on the Debye length scale. Therefore our chosen initial fluctuation as a localized seed is

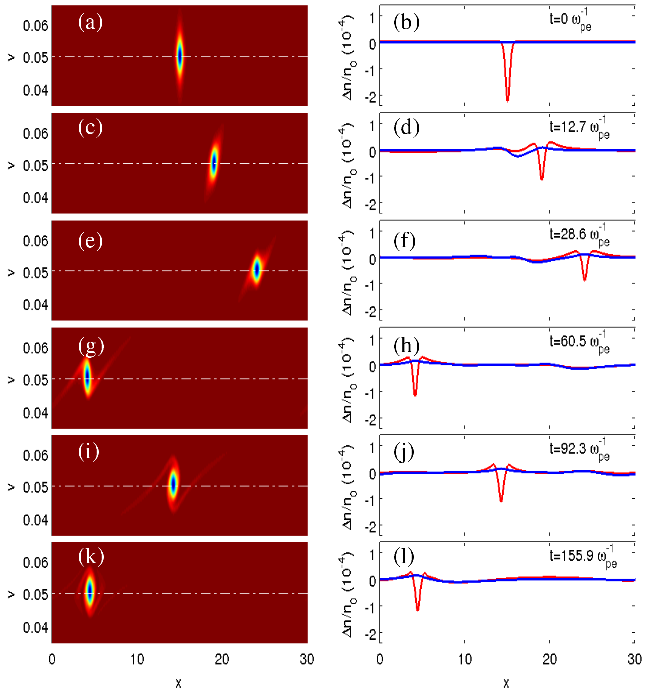

FIG. 1: Evolution of the electron phase-space perturbation and the density perturbations initially introduced at $(x_1, v_1) = (15, 0.05)$.

by no means special but carries the necessary information for subcritical plasma destabilization such as: $|f_1'(x,v,0)|$ being no longer small against $|f_0'(v)|$, a property of the perturbation that we address as non-topological. Under these circumstances linear theory, being still the major theory for the bulk of plasma physics according to which no structures should survive in the subcritical regime, is violated. The present simulations therefore presents the formation of electron hole structures in the subcritical regime and also indicates a gap of existence for the electron hole solutions which is now addressed well within the analytic model for equilibrium solutions of the Vlasov-Poisson system presented by Schamel where the trapped particle effects are retained in distributions.

III. ANALYTICAL MODEL FOR ELECTRON HOLE SOLUTION

With extendability of the fundamental model of trapped species distribution f_{st} to more deterministic forms (discussed further below), the distributions $f_{i,e}$ are written by Schamel as function of total energy $\varepsilon_{i.e}$, hence satisfying the Vlasov equation (see [20] and references therein).

$$f_e(x,v) = \frac{1+k_0^2\psi/2}{\sqrt{2\pi}}\left(\Theta(\epsilon)\exp[-\frac{1}{2}(\sigma\sqrt{2\epsilon}-\tilde{v}_D)^2] + \Theta(-\epsilon)\exp(-\frac{\tilde{v}_D^2}{2})\exp(-\beta\epsilon)\right).$$

In this equation $\Theta(x)$ represents the Heavyside step function, $\sigma = sg(v)$ is the sign of the velocity, $\epsilon := \frac{v^2}{2} - \Phi(x)$ is the single particle energy and $\tilde{v}_D := v_D - v_0$. We note that $f(x,v)$ is a function of two constants of motion, ϵ and σ, which is a necessary requisite for the propagation of a wave, when $\tilde{v}_D > 0$. The first part in (4) represents the free, the second part the trapped electrons. Similarly one can write the distribution function for ion also [20]. Although their distribution can in principle be chosen arbitrarily, see [24], we prefer here a distribution, which is continuous at the separatrix $\epsilon = 0$ and has regularly trapped electrons. Using them in Poisson's equation one can derive the nonlinear dispersion relation (NDR) (see equation (24) of [25]),

$$k_0^2 - \frac{1}{2}Z_r'\left(\tilde{v}_D/\sqrt{2}\right) - \frac{\theta}{2}Z_r'\left(u_0/\sqrt{2}\right) = \frac{16}{15}\left[\frac{3}{2}b(\alpha,u_0)\theta^{3/2} + b(\beta,\tilde{v}_D)\right]\psi^{1/2},$$

where $Z_r(x)$ is the real part of the plasma dispersion function, $\tilde{v}_D := v_D - v_0$ and v_D describes a given constant drift between electron and ion existing already in unperturbed state. The quantity b is function of trapping parameters β

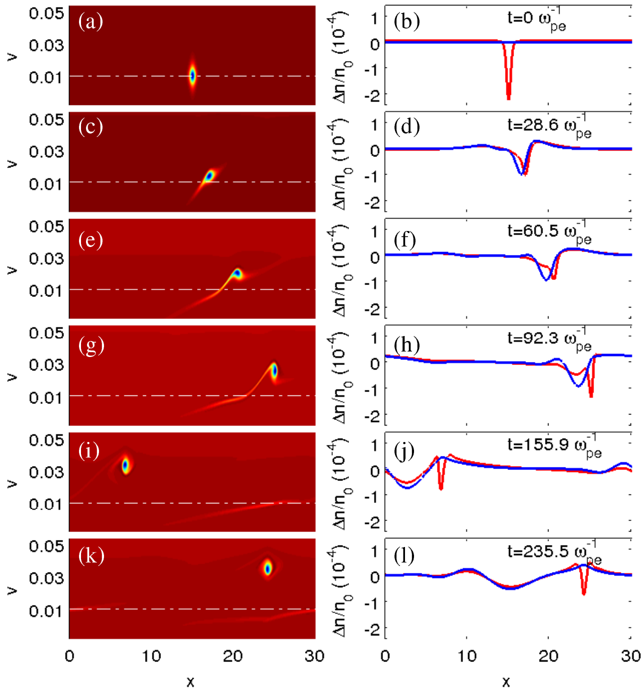

FIG. 2: Evolution of the electron phase-space perturbation and density perturbations initially introduced at $(x_1, v_1) = (15, 0.01)$.

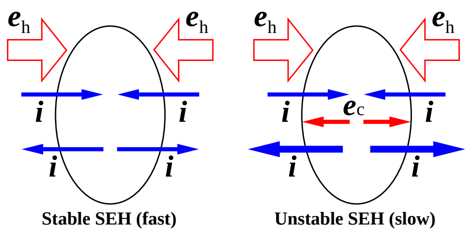

FIG. 3: Schematic of (left) valid fast SEH with $v_0 \geq 0.028$ (right) unstable slow SEH in the forbidden regime $v_0 < 0.028$.

(or α) of electrons (or ions), and has the form

$$b(\beta, \tilde{v}_D) = \frac{1}{\sqrt{\pi}} \left(1 - \beta - \tilde{v}_D^2\right) \exp(-\tilde{v}_D^2/2)$$

such that $b(\alpha, u_0) = 0$ for no trapping effects of ions. The NDR (4) determines the phase velocity of structures (v_0 or u_0) in terms of v_D, k_0^2, θ, ψ, α and β.

In generality, we meet a two parametric solution (described by the parameters k_0^2 and $B = \frac{16}{15} b(\beta, \tilde{v}_D)\sqrt{\psi}$), which is termed cnoidal electron hole (CEH) because it can be expressed by Jacobian elliptic functions such as $cn(x)$ or $sn(x)$. It incorporates as special cases the familiar solitary electron hole (SEH), when $k_0^2 = 0$ and $B > 0$ [26; 27], the harmonic wave, when $B = 0$, as well as the special solitary potential dip (SPD), when $k_0^2 = -\frac{4B}{2} > 0$ demanding $B < 0$. The Compliance with the NDR (4) ensures the net charge flux balance resulting in time independent solutions in the frame of structures. The structure stability (time independence) is therefore subject to its parameters satisfying Eq. (4).

A. Existence of solitary electron hole solution

We now validate holes settled in equilibrium states as described by above analytic model. Since our code is periodic the lowest available wavenumber is $k_0 = \frac{2\pi}{L} = 0.21$, ($k_0^2 = 0.04$), to approximate SEH with. We moreover recognize that both v_D and v_0, and hence $\tilde{v}_D$, are small quantities such that $-\frac{1}{2}Z_r'(\tilde{v}_D/\sqrt{2}) \approx 1$ to a good approximation, while noticing that $Z_r'(x)$ is an even function. Under these special conditions our NDR simplifies and becomes, in case of negligible ion trapping:

$$-\frac{1}{2}Z_r'(u_0/\sqrt{2}) = \frac{1}{\theta}[B - (1+k_0^2)] \equiv \frac{B - 1.04}{10} =: D \tag{4}$$

An inspection of the $-\frac{1}{2}Z_r'(x)$ shows (see Fig. 1 of [20]) that D is negative, corresponding to $1.307 < u_0$, provided that $0 < B < 1.04$. Taking the ideal SEH solution, $\phi(x) = \psi\text{sech}^4(\frac{x}{\Delta})$ with $\Delta = \frac{4}{\sqrt{B}}$, this amounts to $\Delta > 3.92$. Since the spatial width of our perturbation is essentially maintained during the evolution we can take the initial width and approximate Δ by $\Delta \approx \frac{1}{k} = 10$ such that B becomes $B \approx 0.16$. On the other hand, B is given in the present situation by $B = \frac{16(1-\beta)\sqrt{\psi}}{15\sqrt{\pi}}$, which gives, for $\psi \approx 10^{-4}$, a value of the electron trapping parameter $\beta \approx -25.6$. Analytically, we hence get a depression of the electron distribution in the resonant or trapping region, as observed. The corresponding phase velocity is for this case with $D \approx -0.09$ is found to be $u_0 \approx 3.7$ or $v_0 \approx 0.027$, i.e. in the observed range.

B. Unstable region of Solitary Electron Hole

The function $-\frac{1}{2}Z_r'(x)$ has a minimum of -0.285 at $x = 1.5$, which corresponds in terms of u_0 in (4) to $u_0 = 2.12$. This yields, by use of (4), $B = -1.81$ which is outside the admissible range of B, $0 < B < 1.04$. There is hence a gap in u_0 in which no equilibrium (quasi) solitary electron hole can exist. The lowest value of B for which a solution exist is $B = 0^+$ corresponding to $D = -0.104$ or $u_{0s} = 1.48$ ($x_s = 1.05$) and $u_{0f} = 3.61$ ($x_f = 2.55$), hence a gap bounded by these slow and fast velocities, $1.48 < u_0 < 3.61$. This explains why a slow perturbation in case 2 ($v_1 = 0.01 \equiv u_1 = 1.36$), which despite acquiring an adiabatic character, cannot settle below $u_0 = 3.61$. It remains to be shown as to why the hole must accelerate, instead of decaying by phase mixing or decelerating. Quantitatively supported by the energy balance presented further below, the mechanism underlying this acceleration is well explained by the simulated phase-space evolution of the hole, illustrated more clearly in the schematic Fig. 3. While the net charge flux is balanced (zero) for the fast moving structures (left), in a slow moving structure (right) the inbound ion flux limited by finite T_e is too weak to balance the outbound ion flux generated by a longer exposure to hole electric field, $\Delta t \sim 4\pi/v_0 k$. With finite trapped electron population, this insufficient ion influx in a slow moving hole is supplemented by the deterministic response of trapped electrons which create an effective flux by beginning to update their phase-space orbits. The spatial distribution of trapped electrons keeps modifying until the saturation, effectively increasing $|\beta|$, and hence increasing the hole velocity [27]. Note that interpreting β^{-1} as trapped electron temperature (i.e. f_{et} a maximum entropy state), lets the EH represent an structure of infinitesimal scale below which no internal phase-space structures are considered. For treating a deterministic (Vlasov) prescription of internally structured finite amplitude EH, this opens possibility of generalizing Schamel approach by defining a multitude of f_{jt}s, $j = e, i$, (in mutual equilibrium, e.g., in phase locked states [28; 29]) with an associated set of βs and αs.

C. Parametric phase of electron hole instability

Additionally seen in our results is a further acceleration continuing beyond $t = 92.3$ ((g),(h) in Fig. 2 where $v_0 = 0.028$ or $u_0 = 3.8$) when B changes sign to become positive. The further increase in v_0 (u_0) at later times is due to an increase of D (decrease of $|D|$) or increase of $B = \frac{16(1-\beta)\sqrt{\psi}}{15\sqrt{\pi}}$. The latter can have two sources, an increase of ψ and an increase of $(1-\beta) = (1+|\beta|)$, corresponding to a deeper (or sharper, with large k) depression in the phase space vortex center. This additional acceleration essentially corresponds to a net imbalance of ion flux across the separatrix of a valid hole ($B > 0$) due to difference in ion density at two ends of the hole, or an ambient ion density gradient, that must cause further trapped electron response, and hence the acceleration. The model [25] can hence explain both, a gap in u_0 and a further acceleration along the fast dispersion branch.

D. Negative energy character of settled hole

As derived in [19; 30; 31] the total energy density w of a SEH carrying plasma is changed by

$$\Delta w = \frac{\psi}{2}[1 + \frac{1}{2}Z_r'\left(\frac{u_0}{\sqrt{2}}\right)(1 - u_0^2)] \tag{5}$$

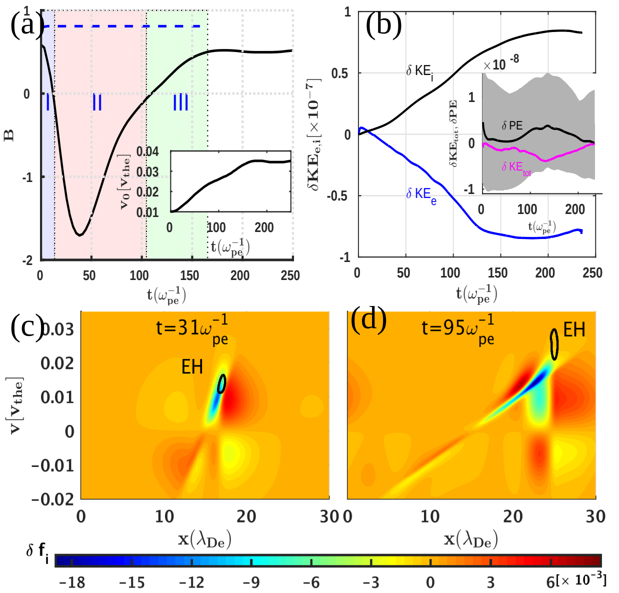

FIG. 4: (a) Time evolution of parameter B and (subplot) velocity v_0 of the SEH. (b) Time variation of change from initial value of kinetic energy of ions (black line), and electrons (blue, averaged over fast electron oscillations). The subplot shows variation of potential (gray and black, total and averaged, respectively) and total kinetic energy (magenta). (c) and (d) δf_i in the ion phase-space at indicated times and black solid line is contour of f_e representing the electron hole.

with respect to the unperturbed, homogeneous state. This expression is negative when it holds: $2.12 < u_0$ (see Fig. 1 of [19]), and is satisfied for all of our settled SEHs. A SEH which is initially placed in an allowed low velocity range ($B > 0$), follows the route of a further release of free energy, moves over the forbidden range and finally settles only in the high energy tail of f_e which are energetically preferred.

IV. IDENTIFICATION OF FORBIDDEN REGION OF EH AND ENERGY EXCHANGE BETWEEN ELECTRON AND ION

In Fig. 4(a) we have presented the time variation of B, calculated using Eq. (4) and rest of the quantities available from the simulation data. This can be noted that for the case 1 (represented by the dashed line) B is uniform and positive at all times as required for the valid SEH eigenmode. For the case 2, however, the value of B (solid line) has negative value in a finite interval (region II) indicating no valid SEH eigenmodes, explaining the unshielded phase of the SEH during this initial interval in case 2. The initial $B > 0$ phase ($t < 10$ or region I) in this case still has an inappropriate SEH eigenmode that violates the negative energy state condition $v_0 \geq 0.016$ as described by (5) [19]. The value of B can still be seen changing once the unshielded phase (region II) is over and $B > 0$ is achieved which is attributed to interaction of valid SEH with the background ion acoustic structure created during the unshielded phase. This is evident from the saturation in the B variation that exactly corresponds to the time of exit of the SEH from the region of a positive ion density gradient ($t \sim 153\omega_{pe}^{-1}$ in Fig. 2 and 4(a)).

We now show that the energy to accelerate ions and growth of an ion acoustic perturbation is derived from the thermal energy of electrons, establishing the unstable hole evolution as a fundamental mechanism for the plasma destabilization driven by a source of free energy. The resulting ion acoustic structure in turn interacts with the SEH and accelerates it further in $B > 0$ regime. This exchange is mediated by the deterministically modifying trapped electron phase-space orbits that allow the electron hole to survive the otherwise expected steady decay of its electric field caused by its unshielded phase.

The steady growth in the ion kinetic energy (δKE$_i$) and a corresponding loss of the averaged thermal energy of the streaming (hot) electrons (δKE$_e$), are plotted in Fig. 4(b) indicating the conversion of δKE$_e$ into δKE$_i$ [31]. This energy exchange is mediated by trapped electrons whose trajectories modify with time, allowing them spend longer time away-from/close-to center in unstable $B < 0$ regime, to supplement the incoming ion flux (pushed by excess thermal electrons) that would balance the outgoing ion flux in a valid plasma eigenmode. The higher $|\beta|$ values correspond to larger dispelled density of trapped electrons and, in turn, to higher hole velocity, explaining the hole acceleration for $t < \tau$, that continues in region III due to coupling with ion density nonuniformity. This conversion of electron thermal energy to ion kinetic energy however need not be 100 % as a fraction of variation in the total thermal energy ($\delta\text{KE}_{\text{tot}} = \delta\text{KE}_e + \delta KE_i$) balances that in the sum (δPE) of electrostatic energies of the SEH and the developing ion compression wave structures (plotted for case 2 in the subplot of Fig. 4(b) as magenta line and black line, respectively). In another study of interaction of two electron holes (not presented here) [**?**] these coherent structures also can exchange energy, momentum between themshelf during interaction. Therefore the coherent structures have a great importance in energy exchange mechanism in hot collisionless plasmas. These results helps for better understanding of energy transport in magnetically confined fusion plasmas. We have also presented the entire process in the ion phase-space by plotting $\delta f_i = f_i - f_{i0}$ at two time points in Fig. 4(c) and (d). The contour of SEH separatrix is superimposed at both the times on the contours of δf_i where an SEH with $B < 0 (t < \tau)$ can be seen coinciding large $\partial \delta f_i / \partial x$, while a valid SEH, with trapped electrons coinciding the ion density hump is seen for $B > 0 (t > \tau)$.

V. SUMMARY AND CONCLUSIONS

To summarize, we have indicated presence of a new forbidden regime of nonlinear electron hole structures at smaller velocities in linearly subcritical collisionless plasmas. We have presented for the first time that a hole structure already in the transient, adiabatic state, follows the cnoidal hole theory represented by a nonlinear dispersion relation and satisfies an energy expression in which the trapping nonlinearity plays the major role. During the unstable region the thermal energy of electron transfer to the thermal energy of ion. This energy exchange mechanism is mediated by the trapped particle structures. These results helps for better understanding of energy transport in magnetically confined fusion plasmas turbulence and formulate better model for intermittent plasma turbulence and anomalous transport.

The evolution is shown to be a manifestation of an already predicted [17] multifaceted nonlinear instability. Importantly, the independence of the nonlinear evolution from the f' and the role of trapped particles that facilitate conversion of thermal energy to coherent modes imply an evolution beyond the realm of linear Landau scenario. Finally we mention that our analysis rests on the availability of a NDR, which is provided by the use of Schamel's kinetically upgraded pseudo-potential method. A BGK-analysis could not be applied because of the lack of a NDR of the latter, which is a consequence of the strong slope singularity of the derived f_{et} within the BGK method [32]. By establishing negative energy SEHs the plasma gains free energy and resides in a metastable, structural thermodynamic state. In the long term run, when dissipative processes are no longer negligible, this enables the plasma to heat electrons and approach the thermodynamic equilibrium state faster than without this intermediate structural state. The latter property is suggested by the existence of separatrices around which collisionality is appreciably enhanced.

References

[1] N. A. Krall and A. W. Trivelpiece, *Principles of Plasma Physics* (San Francisco Press Inc., San Francisco, 1986).
[2] B. D. Fried and R. W. Gould, Phys. Fluids **4**, 139 (1961).
[3] P. Petkaki, M. P. Freeman, T. Kirk, C. E. J. Watt, and R. B. Horne, J. Geophys. Res. **111**, A01205 (2006).
[4] A. Osmane, D. L. Turner, L. B. W. III, A. P. Dimmock, and T. I. Pulkkinen, The Astrophysical Journal **846**, 1 (2017).
[5] K. Saeki, P. Michelsen, H. L. Pécseli, and J. J. Rasmussen, Phys. Rev. Lett. **42**, 501 (1979).
[6] W. Fox, M. Porkolab, J. Egedal, N. Katz, and A. Le, Phys. Rev. Lett. **101**, 255003 (2008).
[7] P. L. Colestock and L. K. Spentzouris, in *AIP Conf. Proc.* (Austin, TX, 1996), 356.
[8] R. H. Berman, D. J. Tetreault, T. H. Dupree, and T. Boutros-Ghali, Phys. Rev. Lett. **48**, 1249 (1982).
[9] M. Lesur, Y. Idomura, and X. Garbet, Phys. Plasmas **16**, 092305 (2009).
[10] H. L. Berk, C. E. Nielsen, and K. V. Roberts, Phys. Fluids **13**, 980 (1970).
[11] M. Lesur and P. H. Diamond, Phys. Rev. E **87**, 031101 (2013).
[12] B. Eliasson and P. K. Shukla, Phys. Rev. Lett. **93**, 045001 (2004).
[13] B. Eliasson and P. K. Shukla, Phys. Reports **422**, 225 (2006).
[14] M. Lesur, P. H. Diamond, and Y. Kosuga, Plasma Phys. Controlled Fusion **56**, 075005 (2014).
[15] T. H. Dupree, Phys. Fluids **26**, 2460 (1983).
[16] I. H. Hutchinson and C. Zhou, Phys. Plasmas **23**, 082101 (2016).
[17] H. Schamel, D. Mandal, and D. Sharma, Phys. Plasmas **24**, 032109 (2017).
[18] I. H. Hutchinson, Phys. of Plasmas **24**, 055601 (2017).
[19] J.-M. Grießmeier and H. Schamel, Phys. Plasmas **9**, 2462 (2002).
[20] H. Schamel, Phys. Plasmas **19**, 020501 (2012).
[21] J. P. Holloway and J. J. Dorning, Phys. Rev. A **44**, 3856 (1991).
[22] L. D. Landau, J. Phys. U.S.S.R. **10**, 25 (1946).
[23] F. Anderegg, C. F. Driscoll, D. H. E. Dubin, and T. M. O'Neil, Phys. Rev. Lett. **102**, 095001 (2009).
[24] H. Schamel, Phys. Plasmas **22**, 042301 (2015).
[25] H. Schamel, Phys. Plasmas **7**, 4831 (2000).

[26] H. Schamel, Physica Scripta. **20**, 306 (1979).
[27] H. Schamel, Physica Scripta. **T2/1**, 228 (1982).
[28] I. Y. Dodin, P. F. Schmit, J. Rocks, and N. J. Fisch, Phys. Rev. Lett. **110**, 215006 (2013).
[29] G. R. Smith and N. R. Pereira, Phys. Fluids **21**, 2253 (1978).
[30] J.-M. Grießmeier, A. Luque, and H. Schamel, Phys. Plasmas **9**, 3816 (2002).
[31] A. Luque and H. Schamel, Phys. Rep. **415**, 261 (2005).
[32] I. B. Bernstein, J. M. Greene, and M. D. Kruskal, Phys. Rev. **108**, 546 (1957).